Available online at www.sciencedirect.com
ScienceDirect
Journal of Sound and Vibration 312 (2008) 476–495
JOURNAL OF SOUND AND VIBRATION
www.elsevier.com/locate/jsvi

Flow-induced instability under bounded noise excitation in cross-flow

Jinyu Zhu[a], X.Q. Wang[b,*], Wei-Chau Xie[a], Ronald M.C. So[b]

[a]*Department of Civil and Environmental Engineering, Faculty of Engineering, University of Waterloo, Waterloo, Ontario, Canada N2L 3G1*
[b]*Department of Mechanical Engineering, The Hong Kong Polytechnic University, Hung Hom, Kowloon,Hong Kong*

Received 27 February 2007; received in revised form 31 May 2007; accepted 26 August 2007

Abstract

Flow-induced vibration of a single cylinder in a cross-flow is mainly due to vortex shedding, which is usually considered as a forced vibration problem. It is shown that flow-induced vibration of a cylinder in the lock-in region is a combination of forced resonant vibration and fluid-damping-induced instability, which leads to time-dependent-fluid-damping-induced parametric resonance and constant-negative-damping-induced instability. The time-dependent fluid damping can be modeled as a bounded noise. The dynamic stability of a two-dimensional system under bounded noise excitation with a narrow-band characteristic is studied through the determination of the moment Lyapunov exponent and the Lyapunov exponent. The case when the system is in primary parametric resonance in the absence of noise is considered and the effect of noise on the parametric resonance is investigated. For small amplitudes of the bounded noise, analytical expansions of the moment Lyapunov exponents and Lyapunov exponents are obtained, which are shown to be in excellent agreement with those obtained using Monte Carlo simulation. The theory of stochastic stability is applied to explore the stability of a cylinder in a cross-flow. The analytical and numerical results show that the time-dependent-fluid-damping-induced parametric resonance could occur, which suggests that parametric resonance also contributes to the vibration of the cylinder in the lock-in range.

1. Introduction

In view of its fundamental importance, vortex-induced vibrations have been studied extensively, using experimental, numerical, and theoretical modeling methods. A number of review articles are available on this subject, e.g., Refs. [1–4]) Since the present study is concerned with the theoretical modeling of vortex-induced vibrations, only relevant work is reviewed and discussed.

Due to the complex nature of fluid–structure interaction in vortex-induced vibration, theoretical modeling is usually carried out in a semi-analytical and semi-empirical way. The developed models can be classified into two groups; one is the force decomposition model, and the other is the wake oscillator model.

*Corresponding author. Tel.: +852 27664502; fax: +852 23654703.
E-mail address: mmxqwang@polyu.edu.hk (X.Q. Wang).

0022-460X/$ - see front matter © 2007 Published by Elsevier Ltd.
doi:10.1016/j.jsv.2007.08.041

In the force decomposition model, the force acting on the cylinder is decomposed into several components representing the forces due to vortex shedding and arising from fluid–structure interaction. This type of model was first proposed by Sarpkaya [5], who divided the total force into a fluid inertia and a fluid damping component. Griffin and Koopmann [6] and Griffin [7] decomposed the total force into a fluid excitation component and a fluid reaction component, the latter representing the force arising from fluid–structure interaction. It was found that fluid damping decreased dramatically in the lock-in range. This implies that fluid damping plays a crucial role in vortex-induced vibration. Based on unsteady flow theory, Chen et al. [8] represented the force arising from the fluid–structure interaction by three linear motion-dependent components, i.e., a fluid inertia, a fluid damping, and a fluid stiffness component. They were combined with a vortex-induced excitation force to give the total force, and Chen et al. [8] concluded that vortex-induced vibration is made up of instability and forced vibration. However, they did not point out explicitly which component is the source that leads to instability.

In the wake oscillator model, a van der Pol oscillator was invoked to represent the dynamics of the lift force due to vortex shedding. It was combined with the equation of motion of the cylinder to form the governing equations for the fluid–structure system. Certain terms related to cylinder motion were assumed in the wake oscillator to represent the effect of structural motion on the lift force, thereby taking the fluid–structure interaction into account. Hartlen and Currie [9] were the first to propose the wake-oscillator model. The model was later modified by a number of researchers, e.g., Skop and Griffin [10], Landl [11], Berger [12], and Balasubramanian and Skop [13], in order to obtain better agreement with experimental measurements and to replicate experimental observations.

Wang et al. [14] proposed a model for vortex-induced vibration in both cross-flow and stream-wise directions. In the model, the quasi-steady flow theory was invoked to account for fluid–structure interactions. This model avoids using the assumed fluid–structure interaction terms as in the wake-oscillator model, but is limited to weak fluid–structure interaction cases only. The reason is because the condition for the quasi-steady flow theory to hold is that the velocity of structural vibration is small compared to the free-stream velocity of the approach flow. If the fluid–structure interaction is strong, the induced structural vibration becomes significant, and the velocity of structural vibration is large, thus the quasi-steady flow theory might not be applicable. An analytical expression of vortex-induced force could be obtained when a linear approximation of fluid–structure interaction was made. This model requires only the parameters for a stationary cylinder compared with the wake-oscillator model, thus avoiding the use of the assumed fluid–structure interaction terms whose coefficients are to be determined from free or forced vibration tests. Using this model, an analytical expression of vortex-induced force could be deduced using a linear approximation of fluid–structure interaction. The expression is similar to that proposed by Sarpkaya [5], but additional nonlinear terms arising from fluid–structure interaction were present. In the Wang et al. [14] model, vortex-induced lift and drag forces acting on the stationary cylinder were represented by sinusoidal functions. The model was modified using the bounded noise process to represent vortex-induced lift and drag forces acting on the stationary cylinder [15] and based on the narrow-band characteristic of the vortex-induced force shown by Vickery and Basu [16]. The modified model was validated against experimental measurements in the literature. The predicted power spectra of the flow-induced force and the cylinder vibration are very similar to experimental results.

In the present study, the model developed by Wang et al. [15] is further extended to include the motion-dependent fluid forces, in an attempt to investigate whether they could induce instability which co-exists with vortex-induced vibration and to identify the source of instability. The motion-dependent forces are taken into account using a linear model proposed by Chen et al. [8], and the vortex shedding forces are modeled by a bounded noise. The resultant model will be analyzed by the determination of Lyapunov exponents and moment Lyapunov exponents which are introduced in Section 2 for stochastically excited systems.

In previous models of vortex-induced vibration, vortex-induced forces are usually represented by sinusoidal functions. However, the shape of the narrow-banded spectrum is very similar to that of a bounded noise (see, e.g., Refs. [16]). Therefore, a bounded noise would be a more appropriate model. In this model, vortex-induced lift and drag forces are modeled by bounded noise processes, while the fluid–structure interaction is accounted for using a quasi-steady flow theory. As a result, the interaction between the drag and lift directions in taken into account. The equations of motion for a cylinder in a cross-flow are set up in Section 3.

Systems excited by stochastic processes in the damping term or stiffness term could become unstable through parametric resonance. Xie [17] studied the parametric stability of a two-dimensional system under real noise excitation. In Section 4, the Lyapunov exponent and moment Lyapunov exponent of the system under bounded noise excitation in the damping term are determined. Analytical results and numerical results are compared to validate the approach.

In Section 5, the results obtained in Section 4 are used to explore the stability of a cylinder in a cross-flow. It is shown that parametric instability could occur, other than the large-amplitude forced vibration, in the lock-in range, which gives more insight into the mechanism of the lock-in phenomenon.

2. Dynamic stability of structures

The equation of motion for many problems of flow-induced vibration is of the general form

$$q''(\tau) + [2\varepsilon_0\beta + \varepsilon_0\mu\varsigma(\tau)]q'(\tau) + \omega_0^2 q(\tau) + f[q, q', \varepsilon_0\varsigma(\tau)] = 0, \tag{1}$$

where the prime denotes differentiation with respect to the time variable τ, q is the generalized coordinate, β the damping constant, ω_0 the circular natural frequency, ε_0 a small fluctuation parameter, $f[q, q', \varepsilon_0\zeta(\tau)]$ a nonlinear function, and $\zeta(\tau)$ a stochastic process describing the random property of the flow

It is natural to ask how the parametric random fluctuation $\zeta(\tau)$ can influence the dynamic stability of system (1). The dynamical stability of the trivial solution of system (1) is governed by the stability of the trivial solution of the linearized equation

$$q''(\tau) + [2\varepsilon_0\beta + \varepsilon_0\mu\varsigma(\tau)]q'(\tau) + \omega_0^2 q(\tau) = 0. \tag{2}$$

The sample or almost-sure stability of the trivial solution of system (2) is determined by the Lyapunov exponent, which characterizes the average exponential rate of growth of the solutions of system (2) for large r and is defined as

$$\lambda_{q(\tau)} = \lim_{\tau\to\infty} \frac{1}{\tau} \log ||\mathbf{q}(\tau)||, \tag{3}$$

where $\mathbf{q}(\tau) = \{q(\tau), q'(\tau)\}^{\mathrm{T}}$ and $||\mathbf{q}|| = (\mathbf{q}^{\mathrm{T}}\mathbf{q})^{1/2}$ is the Euclidean norm. If the largest Lyapunov exponent is negative, the trivial solution of system (2) is stable with probability 1; otherwise, it is unstable almost surely

On the other hand, the stability of the pth moment $E[||\mathbf{q}||^p]$ of the solution of system (2) is governed by the pth moment Lyapunov exponent defined by

$$\Lambda_{q(\tau)}(p) = \lim_{\tau\to\infty} \frac{1}{\tau} \log\, \mathrm{E}[||\mathbf{q}(\tau)^p||], \tag{4}$$

where $E[\cdot]$ denotes the expected value. If $\Lambda_{q(r)}(p)$ is negative, then the pth moment is stable; otherwise, it is almost surely unstable.

The relationship between the sample stability and the moment stability was formulated by Arnold [18]. The pth moment Lyapunov exponent $\Lambda_{q(r)}(p)$ is a convex analytic function in p that passes through the origin and the slope at the origin is equal to the largest Lyapunov exponent $\lambda_{q(\tau)}$, i.e.

$$\lambda_{q(\tau)} = \lim_{p\to\infty} \frac{\Lambda_{q(\tau)}(p)}{p}. \tag{5}$$

The moment Lyapunov exponents are important in obtaining a complete picture of the dynamic stability of the trivial solution of system (2). Suppose the largest Lyapunov exponent $\lambda_{q(\tau)}$ is negative, implying that the trivial solution of system (2) is sample stable, the pth moment typically grows exponentially for large enough p, implying that the pth moment of the trivial solution is unstable. This can be explained by large deviation. Although the solution of the system $||\mathbf{q}||$ goes to zero as time τ approaches infinity with probability one at an exponential rate $\lambda_{q(\tau)}$, there is small probability that $||\mathbf{q}||$ is large, which makes the expected value $E[||\mathbf{q}||^p]$ of this rare event large for large enough values of p, leading to the pth moment instability.

A systematic study of moment Lyapunov exponents is presented by Arnold et al. [19] for linear Itô systems and by Arnold et al. [20] for linear stochastic systems under real noise excitations. A systematic presentation of

the theory of random dynamical systems and a comprehensive list of references are provided by Arnold [21]. The theory and techniques of studying the stability of stochastic systems are presented in Ref. [22].

3. Equations of motion of a single cylinder in a cross-flow

Consider an elastically supported rigid cylinder in a cross flow. The approaching flow is assumed to be uniform and two dimensional. The equations of motion of the cylinder can be written as

$$\ddot{X}(t) + 2\zeta_s\omega_0\dot{X}(t) + \omega_0^2 X(t) = \frac{F^X(t)}{M}, \tag{6a}$$

$$\ddot{Y}(t) + 2\zeta_s\omega_0\dot{Y}(t) + \omega_0^2 X(t) = \frac{F^Y(t)}{M}, \tag{6b}$$

where $X(t)$ and $Y(t)$ are cylinder displacements in the stream-wise and the cross-flow directions, respectively, ω_0 is the natural frequency, ζ_s is the structural damping coefficient, and M is the mass per unit length of the cylinder.

In Eqs. (6a, b), $F^X(t)$ and $F^Y(t)$ are flow-induced forces per unit length acting on the cylinder in the stream-wise and the cross-flow directions, respectively. For the present case, flow-induced forces may be divided into two components: one arising from vortex shedding, and the other due to the feedback effect of cylinder motion. Hence, they can be written as

$$F^X(t) = F_V^X(t) + F_M^X(t), \tag{7a}$$

$$F^Y(t) = F_V^Y(t) + F_M^Y(t), \tag{7b}$$

where the subscripts 'V' and 'M' represent 'vortex-induced' and motion-dependent', respectively.

When the cylinder is stationary, the motion-dependent fluid forces, $F_M^X(t)$ and $F_M^Y(t)$, are absent, and only vortex-induced forces are applied to the cylinder. These are denoted as $F_{V_0}^X(t)$ and $F_{V_0}^Y(t)$ in order to differentiate them from their counterparts when the cylinder is in motion. Once the cylinder is vibrating under the action of vortex-induced forces, its motion can alter vortex shedding, thus changing vortex-induced forces not only in their magnitudes but also in their dominant frequencies.

In addition to vortex-induced excitation, fluid flow will also affect the dynamics of the cylinder in the form of added mass, fluid damping, etc. They are all included into the motion-dependent forces, $F_M^X(t)$ and $F_M^Y(t)$, in the present formulation.

In general, both vortex-induced and motion-dependent forces are nonlinear and dependent on a number of parameters, such as the Reynolds number, the reduced velocity, structural damping, and their expression are complex. In order to carry out a theoretical analysis, approximate modeling is necessary.

3.1. Modeling of vortex-induced forces

In the present study, a model proposed by Wang et al. [15] is invoked for vortex-induced forces. In the model, vortex-induced forces acting on a vibrating cylinder are modeled based on the quasi-steady flow theory, and the basic idea is illustrated in Fig. 1. When the velocity of cylinder vibration is small compared with the flow velocity, the quasi-steady theory is valid. Vortex-induced forces acting on a vibrating cylinder are equal to those acting on the same but stationary cylinder at the instantaneous position, with the direction of the approach flow changed by the velocity of cylinder vibration. Vortex-induced forces are thus expressed as:

$$F_V^X(t) = F_{V_0}^X(t)\cos\theta(t) + F_{V_0}^Y(t)\sin\theta(t), \tag{8a}$$

$$F_V^Y(t) = F_{V_0}^Y(t)\cos\theta(t) + F_{V_0}^X(t)\sin\theta(t), \tag{8b}$$

where θ is the angle between the x-axis and the instantaneous velocity vector of cylinder vibration given by

$$\theta(t) = \tan^{-1}\frac{\dot{Y}}{U - \dot{X}}. \tag{9}$$

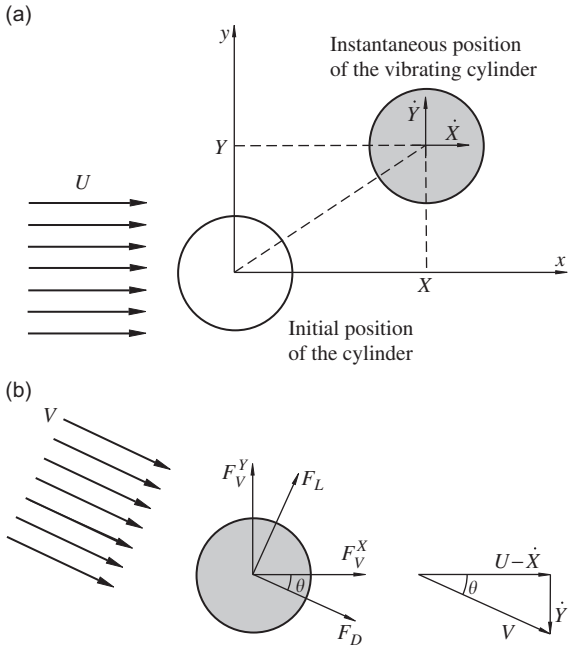

Fig. 1. Illustration of the quasi-steady flow theory: (a) a cylinder subjected to a cross flow; (b) vortex-induced forces acting on the vibrating cylinder according to the quasi-steady flow theory.

In Eqs. (8a, b), $F^X_{V_0}(t)$ and $F^Y_{V_0}(t)$ are the drag and lift forces acting on the stationary cylinder subjected to a cross flow of free-stream velocity $V(t)=\sqrt{(U-\dot{X})^2+\dot{Y}^2}$ at the angle θ. When the cylinder velocity is much smaller than the flow velocity, i.e., $\dot{X}(t)\ll U$ and $\dot{Y}(t)\ll U$,

$$V(t)=\sqrt{(U-\dot{X})^2+\dot{Y}^2}\approx U. \tag{10}$$

Therefore, the lift and drag forces acting on the stationary cylinder can be used to deduce vortex-induced forces applied to the vibrating cylinder. In the literature, the lift and drag forces are usually represented by sinusoidal functions at the Strouhal and the double Strouhal frequencies, respectively. However, Vickery and Basu [16] have shown that the spectrum of vortex-induced force is of narrow-band, even though the approaching flow is uniform. Wang et al. [15] showed that the bounded noise process has similar spectral distribution to that of the vortex-induced force, and is thus appropriate for the force modeling. Using the bounded noise process, the drag and lift forces acting on the stationary cylinder can be expressed as

$$F^X_{V_0}(t)=F_D(t)=\tfrac{1}{2}\rho U^2 D\bar{C}_D+\tfrac{1}{2}\rho U^2 D C_D\cos[\nu_D t+\sigma_D W(t)+\phi_D], \tag{11a}$$

$$F^Y_{V_0}(t)=F_L(t)=\tfrac{1}{2}\rho U^2 D C_L\cos[\nu_L t+\sigma_L W(t)+\phi_L], \tag{11b}$$

where ρ is the density of the fluid, $\bar{C}_D$ is the mean drag coefficient, $C_D(C_L)$ is the amplitude of the fluctuating drag(lift) coefficients, $\nu_D(\nu_L)$ and $\sigma_D(\sigma_L)$ are the frequency and bandwidth of the vortex-induced force in the drag(lift) direction, respectively, $W(t)$ is the standard Wiener process, and ϕ_D and ϕ_L are uniformly distributed random numbers to make the bounded noise processes stationary.

In general, an iteration process is needed to obtain the expressions of vortex-induced forces using Eqs. (8a, b) since the flow-induced forces and the cylinder vibrations have an interactive relationship through the angle θ, which is nonlinearly related to cylinder motion. For small amplitude vibration, however, a linear

approximation can be invoked in the present study, i.e.,

$$\sin\theta(t) = \frac{\dot{Y}(t)}{\sqrt{[U-\dot{X}(t)]^2 + \dot{Y}^2(t)}} \approx \frac{\dot{Y}(t)}{U}, \tag{12a}$$

$$\cos\theta(t) = \frac{U-\dot{X}(t)}{\sqrt{[U-\dot{X}(t)]^2 + \dot{Y}^2(t)}} \approx 1. \tag{12b}$$

It follows then that the vortex-induced forces can be expressed as

$$F_V^X(t) = F_D(t) + F_L(t)\frac{\dot{Y}(t)}{U}, \tag{13a}$$

$$F_V^Y(t) = F_L(t) - F_D(t)\frac{\dot{Y}(t)}{U}, \tag{13b}$$

Substituting Eqs. (13a, b) into Eqs. (6a, b), the equations of motion are written as

$$\ddot{X}(t) + 2\zeta_s\omega_0\dot{X}(t) + \omega_0^2 X(t) = \frac{1}{M}\left[F_D(t) + F_L(t)\frac{\dot{Y}(t)}{U} + F_M^X(t)\right], \tag{14a}$$

$$\ddot{Y}(t) + 2\zeta_s\omega_0\dot{Y}(t) + \omega_0^2 Y(t) = \frac{1}{M}\left[F_L(t) + F_D(t)\frac{\dot{Y}(t)}{U} + F_M^Y(t)\right]. \tag{14b}$$

Since the present study is focused on the cylinder vibration in the cross-flow direction, only Eq. (14b) is retained and re-written as

$$\ddot{Y}(t) + \left[2\zeta_s\omega_0 + \frac{1}{M}\frac{F_D(t)}{U}\right]\dot{Y}(t) + \omega_0^2 Y(t) = \frac{1}{M}\left[F_L(t) + F_M^Y(t)\right]. \tag{15}$$

3.2. Modeling of motion-dependent forces

Cylinder vibration also induces other fluid forces, such as the added mass and the fluid damping force, which are not considered in the above model. In the present study, they are included in the motion-dependent fluid force as

$$F_M^Y = -\frac{\rho\pi D^2}{4}c_m\ddot{Y} + \frac{\rho U^2}{\bar{\omega}_0}c_d\dot{Y} + \rho U^2 c_k Y, \tag{16}$$

where c_m, c_d, and c_k are the added mass, the fluid damping, and the fluid stiffness coefficients, respectively, and $\bar{\omega}_0$ is the natural frequency of the system, whose expression is given in Section 3.3. In general, $c_m = 1$ since the added mass is considered to be equal to the mass of fluid displaced by the vibrating cylinder. As a first approximation, the fluid damping force is assumed to be proportional to the velocity of cylinder vibration. The fluid stiffness term only affects the natural frequency of the fluid–structure system.

3.3. Model for vortex-induced vibration

Substituting Eq. (16) into Eq. (15) yields

$$\begin{aligned}\ddot{Y}(t) + \left[2\zeta_s\omega_0 + \frac{1}{M}\frac{F_D(t)}{U}\right]\dot{Y}(t) + \omega_0^2 Y(t) \\ = \frac{1}{M}\left[F_L(t) - \frac{\rho\pi D^2}{4}c_m\ddot{Y} + \frac{\rho U^2}{\bar{\omega}_0}c_d\dot{Y} + \rho U^2 c_k Y\right].\end{aligned} \tag{17}$$

After some manipulation, Eq. (17) can be written as

$$\left(M+\frac{\rho\pi D^2}{4}\right)\ddot{Y}(t)+\left[2\zeta_s\omega_0 M+\frac{F_D(t)}{U}-\frac{\rho U^2}{\bar{\omega}_0}c_d\right]\dot{Y}(t)+(M\omega_0^2-\rho U^2 c_k)Y(t)=F_L(t). \tag{18}$$

Using Eqs. (11a, b), Eq. (18) can be simplified as

$$\ddot{Y}(t)+\left\{2\bar{\zeta}_s\bar{\omega}_0+\frac{U[\bar{C}_D+C_D\cos\eta_D(t)]}{2DM_r}-\frac{U^2}{\bar{\omega}_0 D^2 M_r}c_d\right\}\dot{Y}(t)+\bar{\omega}_0^2 Y(t)=\frac{U^2}{2DM_r}C_L\cos\eta_L(t), \tag{19}$$

where

$$\bar{M}=M+\frac{\rho\pi D^2}{4},\quad M_r=\frac{\bar{M}}{\rho D^2},$$

$$\bar{\omega}_0=\sqrt{\frac{M\omega_0^2-\rho U^2 c_k}{\bar{M}}},\quad \bar{\zeta}_s=\frac{\omega_0 M}{\bar{\omega}_0\bar{M}}\zeta_s,$$

$$\eta_D(t)=\nu_D t+\sigma_D W(t)+\phi_D,\quad \eta_L(t)=\nu_L t+\sigma_L W(t)+\phi_L.$$

Non-dimensionalizing Eq. (19) with respect to U and D, and applying the time scaling $\tau=\bar{\omega}_0 t$, the equation becomes

$$Y''(\tau)+\left[2\bar{\zeta}_s+\frac{\bar{U}_{r0}}{2\pi}\frac{\bar{C}_D+C_D\cos\tilde{\eta}_D(\tau)}{2M_r}-\frac{\bar{U}_{r0}^2}{4\pi^2}\frac{c_d}{M_r}\right]Y'(\tau)+Y(\tau)=\frac{\bar{U}_{r0}^2}{4\pi^2}\frac{C_L}{M_r}\cos\tilde{\eta}_L(\tau), \tag{20}$$

where

$$\bar{U}_{r0}=\frac{2\pi U}{\bar{\omega}_0 D}=\text{the reduced velocity},$$

$$\tilde{\eta}_D(t)=\tilde{\nu}_D t+\tilde{\sigma}_D W(t)+\phi_D,\quad \tilde{\nu}_D=\frac{\nu_D}{\bar{\omega}_0},\quad \tilde{\sigma}_D=\frac{\sigma_D}{\sqrt{\bar{\omega}_0}},$$

$$\tilde{\eta}_L(t)=\tilde{\nu}_L t+\tilde{\sigma}_L W(t)+\phi_L,\quad \tilde{\nu}_L=\frac{\nu_L}{\bar{\omega}_0},\quad \tilde{\sigma}_L=\frac{\sigma_L}{\sqrt{\bar{\omega}_0}}.$$

Letting

$$\beta=2\bar{\zeta}_s+\frac{\bar{U}_{r0}}{2\pi}\frac{\bar{C}_D}{2M_r}-\frac{\bar{U}_{r0}^2}{4\pi^2}\frac{c_d}{M_r},\quad \mu_D=\frac{\bar{U}_{r0}}{2\pi}\frac{C_D}{M_r},$$

$$\mu_L=\frac{\bar{U}_{r0}^2}{4\pi^2}\frac{C_L}{M_r}. \tag{21}$$

Eq. (20) can be written as

$$Y''(\tau)+[\beta+\mu_D\cos\tilde{\eta}_D(\tau)]Y'(\tau)+Y(\tau)=\mu_L\cos\tilde{\eta}_L(\tau). \tag{22}$$

From Eq. (22), one can see that two sources are responsible for cylinder vibration: $\mu_L\cos\tilde{\eta}_L(\tau)$, which may lead to the main resonance if $\tilde{\nu}_L=\nu_L/\bar{\omega}_0=1$, and $\beta+\mu_D\cos\tilde{\eta}_D(\tau)$, which may give rise to a negative-damping-induced instability or a parametric instability depending on the relationship between β, μ_D, and $\tilde{\eta}_D(\tau)$. This is studied in detail in the following section.

4. Stability of a two-dimensional system under stochastic parametric excitation

For a single degree-of-freedom system described by (22), there exist two types of excitations: the forcing excitation $\mu_L\cos\tilde{\eta}_L(\tau)$ on the RHS of the equation and the parametric excitation on the LHS of the equation. The forcing excitation induces main resonance when its frequency is close to the natural frequency of the

system, at which point large amplitude vibration occurs when the system damping is small. In particular, if the system is undamped, the amplitude of response grows linearly with time.

The significance of the parametric excitation depends on the damping of the system, $\beta + \mu_D \cos \tilde{\eta}_D(\tau)$. The system damping consists of a constant component and a time-dependent component expressed in the form of a bounded noise. When the constant system damping β is negative, the system becomes unstable regardless of the value of $\mu_D \cos \tilde{\eta}(\tau)$. It can be seen that β is related to three quantities: the structural damping ζ_s, the mean drag coefficient $\bar{C}_D$, and the motion-dependent fluid damping c_d. Both ζ_s and $\bar{C}_D$ are positive and their effect is to increase the system damping, thus would not induce unstable motion of the system. The one which may induce negative system damping is the fluid damping coefficient c_d. The condition for $\beta < 0$ is given by

$$c_d > \frac{4\pi^2 M_r}{U_r^2}\left(2\bar{\zeta}_s + \frac{\bar{U}_{r0}}{2\pi}\frac{\bar{C}_D}{2M_r}\right). \tag{23}$$

Eq. (23) shows that once c_d is large enough, the system becomes unstable. Such instability can be termed as a constant-fluid-damping-induced instability.

When β is positive and its absolute value is larger than μ_D ($\beta > \mu_D$), the system is stable. In this case, the resonance plays a dominant role in the response. When β is positive and its value is smaller than μ_D ($\beta > \mu_D$), the stability of the system depends on the time-dependent fluid-damping component $\mu_D \cos \tilde{\eta}(\tau)$, Whatever value β might have, the time-dependent fluid-damping component $\mu_D \cos \tilde{\eta}(\tau)$, always tends to destabilize the system provided that its dominant frequency is in the vicinity of twice the natural frequency of the system. Parametric instability is induced, and the amplitude of cylinder vibration grows exponentially even in the presence of damping. In this case, parametric resonance becomes more pronounced than the main resonance. The theory of stochastic instability has to be used to investigate the parametric stability of the system, as given below. Since the forcing term does not affect the parametric instability, it is dropped in the following analysis.

4.1. Formulation

Consider the dynamic behavior of the following parametrically excited, two-dimensional system

$$\frac{\mathrm{d}^2 q(\tau)}{\mathrm{d}\tau^2} + [2\varepsilon_0\beta + \varepsilon_0\mu\cos\eta(\tau)]\frac{\mathrm{d}q(\tau)}{\mathrm{d}\tau} + \omega_0^2 q(\tau) = 0,$$

$$n(\tau) = v_0\tau + \sigma_0 W(\tau) + \theta \tag{24}$$

in which $\cos\eta(\tau)$ is a bounded noise, and θ is a uniformly distributed random number in $(0, 2\pi)$ that makes $\cos\eta(\tau)$ a stationary process.

For the two-dimensional system (24), the damping term can be removed by the transformation $q(\tau) = x(\tau)e^{-\varepsilon_0\beta\tau}$ and further simplified using the time scaling $t = \omega\tau$ where $\omega^2 = \omega_0^2 - \omega_0^2\beta^2$, to yield

$$\frac{\mathrm{d}^2 x(t)}{\mathrm{d}t^2} + \varepsilon\mu\cos\tilde{\eta}(t)\frac{\mathrm{d}x(t)}{\mathrm{d}t} + [1 - \varepsilon^2\mu\beta\cos\tilde{\eta}(t)]x(t) = 0, \quad \mathrm{d}\tilde{\eta}(t) = v\mathrm{d}t + \sigma\mathrm{d}W(t),$$

where $\varepsilon = \varepsilon_0/\omega$, $v = v_0/\omega$, and $\sigma = \sigma_0/\sqrt{\omega}$. The Lyapunov exponents and the moment Lyapunov exponents of systems (24) and (25) are related by

$$\lambda_{q(\tau)} = -\varepsilon_0\beta + \omega\lambda_{x(t)}, \quad \Lambda_{q(t)}(p) = -p\cdot\varepsilon_0\beta + \omega\Lambda_{x(t)}(p).$$

In the absence of noise, i.e. when $a = 0$, the bounded noise reduces to a sinusoidal function and system (25) is in primary parametric resonance when v is in the vicinity of 2 (see, e.g., Ref. [22]). In order to have an understanding of the effect of noise on the parametric resonance, it is important and interesting to study the dynamic stability of system (25) under the excitation of a narrow-band process about $v = 2$, which can be achieved with the bounded noise for small values of σ.

Hence, the following two-dimensional system under bounded noise excitation is considered

$$\frac{\mathrm{d}^2 y(t)}{\mathrm{d}t^2} + \varepsilon\mu\cos\eta(t)\frac{\mathrm{d}y(t)}{\mathrm{d}t} + [1 - \varepsilon^2\mu\beta\cos\eta(t)]y(t) = 0, \quad \mathrm{d}\eta(t) = v\mathrm{d}t + \varepsilon^{1/2}\sigma\,\mathrm{d}W(t). \tag{26}$$

The introduction of the scaling parameter $\varepsilon^{1/2}$ in the noise fluctuation term $\sigma \mathrm{d}W(t)$ renders the bounded noise a narrow-band process for $\varepsilon = o(1)$ and $a = \mathcal{O}(1)$.

The eigenvalue problem governing the moment Lyapunov exponent of system (26) can be set up using Wedig's approach [23]. System (26) can be rewritten as a three-dimensional system

$$\mathrm{d}\begin{Bmatrix} y_1 \\ y_2 \\ \eta \end{Bmatrix} = \begin{Bmatrix} -[1-\varepsilon^{y_2}\mu\beta\cos\eta]y_1 - \varepsilon\mu\eta y_2 \end{Bmatrix}\mathrm{d}t + \begin{Bmatrix} 0 \\ 0 \\ \varepsilon^{1/2}\sigma \end{Bmatrix}\mathrm{d}W.$$

Khasminskii's transformation

$$\cos\varphi = \frac{y_1}{a}, \quad \sin\varphi = y_2/a \quad a = ||\mathbf{y}|| = (y_1^2 + y_2^2)^{1/2}$$

can be applied to transform the Cartesian coordinates (y_1, y_2) to the polar coordinates (a, φ), and the pth norm of $\mathbf{y}$ is defined as $P = a^p$. The Itô equations for P and φ can be derived using Itô's Lemma

$$\mathrm{d}P = pP\sin\varphi\cos\eta(-\varepsilon\mu\sin\varphi + \varepsilon^2\beta\mu\cos\varphi)\,\mathrm{d}t,$$

$$\mathrm{d}\varphi = (-1 - \varepsilon\mu\sin\varphi\cos\varphi\cos\eta + \varepsilon^2\mu\beta\cos^2\varphi\cos\eta)\,\mathrm{d}t.$$

Applying a linear stochastic transformation

$$S = T(\eta,\varphi)P, \quad P = T^{-1}(\eta,\varphi)S, \quad -\infty < \eta < +\infty, \quad 0 \leqslant \varphi < \pi,$$

the Itô equation for the transformed pth norm process S can also be derived using Itô's Lemma

$$\mathrm{d}S = \left[\frac{1}{2}\varepsilon\sigma^2 T_{\eta\eta} + vT_\eta - (1 + \varepsilon\mu\ \sin\ \varphi\ \cos\ \varphi\ \cos\eta - \varepsilon^2\mu\beta\cos^2\varphi\ \cos\eta)T_\varphi \right.$$
$$\left. + pP\sin\ \varphi\ \cos\ \eta(-\varepsilon\mu\ \sin\ \varphi + \varepsilon^2\beta\mu\ \cos\ \varphi)T\right]p\mathrm{d}t + \varepsilon^{1/2}\sigma T_\eta p\mathrm{d}W. \tag{27}$$

For bounded and non-singular transformation $T(\eta,\varphi)$, both processes P and S are expected to have the same stability behavior. Therefore, $T(\eta,\varphi)$, is chosen so that the drift term of the Itô differential equation (27) is independent of the noise process $\eta(t)$ and the phase process so φ that

$$\mathrm{d}S = \Lambda S\,\mathrm{d}t + \varepsilon^{1/2}\sigma T_\eta T^{-1} S\mathrm{d}W. \tag{28}$$

Comparing Eqs. (28) and (27), it is seen that such a transformation $T(\eta,\varphi)$, is given by the following equation:

$$\tfrac{1}{2}\varepsilon\sigma^2 T_{\eta\eta} + vT_\eta - (1 + \varepsilon\mu\sin\varphi\cos\varphi\cos\eta - \varepsilon^2\mu\beta\cos^2\varphi\cos\eta)T_\varphi$$
$$+ pP\ \sin\ \varphi\cos\eta\,(-\varepsilon\mu\sin\varphi\ + \varepsilon^2\beta\mu\cos\varphi)T = \Lambda T, \quad -\infty < \eta < +\infty, \quad 0 \leqslant \varphi < \pi \tag{29}$$

in which $T(\eta,\varphi)$ is a periodic function in φ of period π and is bounded when $\eta \to \pm\infty$ Eq. (29) defines an eigenvalue problem of a second-order differential operator with Λ being the eigenvalue and $T(\eta,\varphi)$ the associated eigenfunction. From Eq. (28), the eigenvalue Λ is seen to be the Lyapunov exponent of the pth moment of system (26), i.e. $\Lambda = \Lambda_{y(t)}(\mathrm{p})$.

4.2. Weak noise expansions of the moment Lyapunov exponent

4.2.1. Perturbation expansion

For weak noise excitation, i.e. for $0 < \varepsilon \ll 1$, perturbation methods can be applied to solve the partial differential eigenvalue problem (29) for the perturbative expansions of the moment Lyapunov exponent $\Lambda_{y(t)}(p)$. Since the small parameter ε appears as a coefficient of the term $T_{\eta\eta}$, a method of singular perturbation (see, e.g., Ref. [24]) must be applied.

Define $v = v_0 + \varepsilon\Delta$, where $v_0 = 2$ corresponds to the primary parametric resonance in the absence of noise and Δ is the detuning parameter. Applying the transformation

$$\eta = \varepsilon^{1/2}\xi - v_0\varphi, \quad \xi = \varepsilon^{-1/2}(\eta + v_0\varphi),$$

Eq. (29) becomes

$$\frac{\sigma^2}{2}T_{\xi\xi} - T_\varphi + \varepsilon^{1/2}\Delta T_\xi + \mu\cos\varphi\cos(\varepsilon^{1/2}\xi - 2\varphi)(-\varepsilon\sin\varphi + \varepsilon^2\beta\cos\varphi)(T_\varphi + 2\varepsilon^{-1/2}T_\xi)$$
$$+ \mu p\sin\varphi\cos(\varepsilon^{1/2}\xi - 2\varphi)(-\varepsilon\sin\varphi + \varepsilon^2\beta\cos\varphi)T = \Lambda T, \tag{30}$$

in which the eigenfunction T is treated as a function of ξ, φ and ε. Denoting $z = \varepsilon^{1/2}\xi$, the eigenfunction $T(\xi, z, \varepsilon.)$ becomes $Y(\xi, z, \varphi)$. It can be shown that

$$T_\xi = Y_\xi + \varepsilon^{1/2}Y_z, \quad T_{\xi\xi} = Y_{\xi\xi} + 2\varepsilon^{1/2}Y_{\xi z} + \varepsilon Y_{zz}. \tag{31}$$

Substituting Eq. (31) into Eq. (30) leads to

$$\mathscr{L}(P)Y = \Lambda_{y(t)}Y, \quad \mathscr{L}(p)Y = \mathscr{L}_0 Y + \varepsilon^{1/2}\mathscr{L}_1 Y + \varepsilon\mathscr{L}_2 Y + \varepsilon^{3/2}\mathscr{L}_3 Y + \varepsilon^2\mathscr{L}_4 Y, \tag{32}$$

where

$$\mathscr{L}_0 Y = \tfrac{1}{2}\sigma^2 Y_{\xi\xi} - Y_\varphi,$$
$$\mathscr{L}_1 Y = \sigma^2 Y_{\xi z} + [\Delta - 2\mu\cos(z - 2\varphi)\sin\varphi\cos\varphi]Y_\xi,$$
$$\mathscr{L}_2 Y = \tfrac{1}{2}\sigma^2 Y_{zz} + \Delta Y_z - \mu\cos(z - 2\varphi)\sin\varphi\cos\varphi(2Y_z + Y_\varphi) - \mu p\cos(z - 2\varphi)\sin^2\varphi Y],$$
$$\mathscr{L}_3 Y = 2\mu\beta\cos(z - 2\varphi)\cos^2\varphi Y_\xi,$$
$$\mathscr{L}_4 Y = \mu\cos\varphi(z - 2\varphi)[\beta\cos\varphi(2Y_z + Y_\varphi) + p\sin\varphi Y],$$

The eigenvalue $\Lambda_{y(t)}(p)$ and the eigenfunction $Y(\xi, z, \varphi)$ can be expanded in powers series of $\varepsilon^{1/2}$ as

$$\Lambda_{y(t)}(p) = \sum_{n=0}^{\infty}\varepsilon^{n/2}\Lambda_n, \quad Y(\xi, z, \varphi) = \sum_{n=0}^{\infty}\varepsilon^{n/2}Y_n(\xi, z, \varphi), \tag{33}$$

where $Y_n(\xi, z, \varphi)$ are periodic functions in φ of period π. Substituting Eqs. (33) into Eq. (32) yields the following sequence of equations:

$$\mathscr{O}(1): \quad \mathscr{L}_0 Y_0 = \Lambda_0 Y_0,$$
$$\mathscr{O}(\varepsilon^{1/2}): \quad \mathscr{L}_0 Y_1 + \mathscr{L}_1 Y_0 = \Lambda_0 Y_1 + \Lambda_1 Y_0,$$
$$\mathscr{O}(\varepsilon^{1}): \quad \mathscr{L}_0 Y_2 + \mathscr{L}_1 Y_1 + \mathscr{L}_2 Y_0 = \sum_{i=0}^{2}\Lambda_i Y_{n-i},$$
$$\mathscr{O}(\varepsilon^{3/2}): \quad \mathscr{L}_0 Y_3 + \mathscr{L}_1 Y_2 + \mathscr{L}_2 Y_1 + \mathscr{L}_3 Y_0 = \sum_{i=0}^{3}\Lambda_i Y_{n-i},$$
$$\mathscr{O}(\varepsilon^{n/2}): \quad \mathscr{L}_0 Y_n + \mathscr{L}_1 Y_{n-1} + \mathscr{L}_2 Y_{n-2} + \mathscr{L}_3 Y_{n-3} + \mathscr{L}_4 Y_{n-4} = \sum_{i=0}^{3}\Lambda_i Y_{n-i} \quad n = 4, 5, \cdots.$$

4.2.2. Zeroth-order perturbation

The zeroth-order perturbation equation is $\mathscr{L}_0\ Y_0 = \Lambda_0\ Y_0$, or

$$\frac{\sigma^2}{2}\frac{\partial^2 Y_0}{\partial\xi^2} - \frac{\partial^2 Y_0}{\partial\varphi} = \Lambda_0 Y_0. \tag{35}$$

Since the moment Lyapunov exponent $\Lambda_{y(t)}(p)$ passes through the origin, i.e.

$$\Lambda_{y(t)}(0) = \Lambda_0(0) + \varepsilon^{1/2}\Lambda_1(0) + \varepsilon\Lambda_2(0) + \cdots = 0,$$

one obtains $\Lambda_0(0) = \Lambda_1(0) = \Lambda_2(0) = \cdots = 0$. Because Eq. (35) does not contain p explicitly, $\Lambda_0(0) = 0$ implies $\Lambda_0(p) = 0$. Applying the method of separation of variables and noting that $Y_0(\xi, z, \varphi) = Y_0(\xi, z, \varphi+\pi)$, one obtains $Y_0(\xi, z, \varphi) = Z_0(z)$, where $Z_0(z)$ is an arbitrary function of z.

The adjoint Equation of Eq. (35) is

$$\frac{\sigma^2}{2}\frac{\partial^2 Y_0^*}{\partial \xi^2} - \frac{\partial^2 Y_0^*}{\partial \varphi} = \Lambda_0 Y_0^*. \tag{35'}$$

Similarly, one can obtain $Y_0^*(\xi, z, \varphi,) = Z_0^*(z)$, where $Z_0^*(z)$ is an arbitrary function of z.

4.2.3. First-order perturbation

Since $\Lambda_0 = 0$, the first-order perturbation equation becomes

$$\mathscr{L}_0 Y_1 = \Lambda_1 Y_0 - \mathscr{L}_1 Y_0. \tag{36}$$

From the Fredholm Alternative, for Eq. (36) to have a non-zero solution, it is required that

$$(\Lambda_1 Y_0 - \mathscr{L}_1 Y_0, \quad Y_0^*) = 0 \tag{37}$$

where (f, g) denotes the inner product of functions $f(\xi, z, \varphi)$ and $g(\xi, z, \varphi)$ defined as

$$(f, g) = \int_{z=-\infty}^{+\infty}\int_{\xi=-\infty}^{+\infty}\int_{\varphi=0}^{\pi} f(\xi, z, \varphi) g(\xi, z, \varphi)\, \mathrm{d}\varphi\, \mathrm{d}\xi\, \mathrm{d}z.$$

Since $Y_0(\xi, z, \varphi) = Z_0(z)$, which leads to $\mathscr{L}_1 Y_0 = 0$, Eq. (37) results in $\Lambda_1(p) = 0$. Eq. (36) then becomes $\mathscr{L}_0 Y_1 = 0$. Following the same procedure as in Section 4.2.2, it is easy to show that $Y_1(\xi, z, \varphi) = Z_1(z)$.

4.2.4. Second-order perturbation

Since $\Lambda_0 = \Lambda_1 = 0$, $\mathscr{L}_1 Y_1 = 0$, the second-order perturbation equation becomes

$$\mathscr{L}_0 Y_2 = \Lambda_2 Y_0 - \mathscr{L}_2 Y_0. \tag{38}$$

From the Fredholm Alternative, for Eq. (38) to have non-trivial solutions, it is required that

$$(\Lambda_2 Y_0 - \mathscr{L}_2 Y_0, \quad Y_0^*) = 0,$$

which can be reduced to

$$\int_{z=-\infty}^{+\infty} Z_0^*(z)\left\{\int_{\varphi=0}^{\pi}\left\{\frac{\sigma^2}{2}\ddot{Z}_0(z) + [\Delta - 2\mu\sin\varphi\cos\varphi\cos(z-2\varphi)]\dot{Z}_0(z) + [-\mu p\sin^2\varphi\cos(z-2\varphi) - \Lambda_2]Z_0(z)\right\}\mathrm{d}\varphi\right\}\mathrm{d}z = 0, \tag{39}$$

Since Eq. (39) holds for arbitrary $Z_0^*(z)$, it results in

$$\tfrac{1}{2}\sigma^2 Z_0^{*}(z) + (\Delta - \tfrac{1}{2}\mu\,\sin\,z)\dot{Z}_0(z) + \left(\tfrac{1}{4}\mu p\,\cos\,z - \Lambda_2\right)Z_0(z) = 0. \tag{40}$$

This is a second-order ordinary differential eigenvalue problem. Λ_2 is the eigenvalue and $Z_0(z)$ is the corresponding eigenfunction. Eq. (40) can be solved using the Fourier series

$$Z_0(z) = C_0 + \sum_{n=1}^{n}(C_n\cos nz + S_n\sin nz), \tag{41}$$

where C_0, C_n, S_n, $n = 1, 2, \ldots, N$, are constant coefficients to be determined. For the calculation efficiency, the Fourier series is truncated to include N sine and cosine terms.

Substituting Eq. (41) into Eq. (40), multiplying the resulting equation by $\cos nz$ and $\sin nz$, for $n = 0, 1, \ldots, N$, respectively, lead to a set of $2N+1$ homogeneous linear algebraic equations for C_0, C_n, S_n, $n = 1, 2, \ldots, N$.

These equations can be written as the matrix form

$$\left[\mathbf{A} - \Lambda_2^{(N)}\mathbf{B}\right]\mathbf{X} = 0, \tag{42}$$

where the superscript "(N)" signifies that the Fourier series is truncated to include N harmonic terms, $\mathbf{X} = \{C_0; C_1, S_1; C_2, S_2; \ldots; C_N, S_N\}^{\mathrm{T}}$,and $\mathbf{A}$, $\mathbf{B}$ are matrices of dimension $(2N+1)\times(2N+1)$.

For system (42) to have non-trivial solutions, the determinant of the coefficient matrix must be zero, i.e.

$$|\mathbf{A} - \Lambda_2^{(N)}\mathbf{B}| = 0,$$

which leads to a polynomial equation for Λ_2 of degree $2N+1$

$$\left[\Lambda_2^{(N)}\right]^{2N+1} + \mathrm{d}_{2N}^{(N)}\left[\Lambda_2^{(N)}\right]^{2N} + \mathrm{d}_{2N-1}^{(N)}\left[\Lambda_2^{(N)}\right]^{2N-1} + \cdots + \mathrm{d}_1^{(N)}\Lambda_2^{(N)} + \mathrm{d}_0^{(N)} = 0. \tag{43}$$

Solving Eq. (43), one can obtain an approximation of $\Lambda_2^{(N)}$. As a result, the moment Lyapunov exponent can be approximated by

$$\Lambda_{y(t)}(p) \approx \varepsilon\Lambda_2^{(N)}. \tag{44}$$

Using Eq. (5), an approximation of the Lyapunov exponent can be easily obtained

$$\lambda_{y(t)} \approx \varepsilon\lambda_2^{(N)}, \quad \lambda_2^{(N)} = \lim_{p\to 0}\frac{\Lambda_2^{(N)}}{p}. \tag{45}$$

Eq. (45) implies that $\Lambda_2^{(N)} = \mathcal{O}(p)$ as $p\to 0$, and hence $\left[\Lambda_2^{(N)}\right]^n = \mathcal{O}(p)$, for $n\geqslant 2$. From Eq. (43), one obtains

$$\lambda_2^{(N)} = -\lim_{p\to 0}\frac{d_0^{(N)}}{d_1^{(N)}p}. \tag{46}$$

Three-dimensional plots of $\Lambda_2^{(N)}$ are shown in Fig. 2 for $\sigma = 1.0$. It is clearly seen that, for small noise fluctuation parameter σ, i.e. when the bounded noise is a narrow-band process, the effect of parametric resonance is very significant. When the value of σ is increased, the bandwidth of the bounded noise process $\eta(t)$ increases, resulting in a less prominent effect of the parametric resonance.

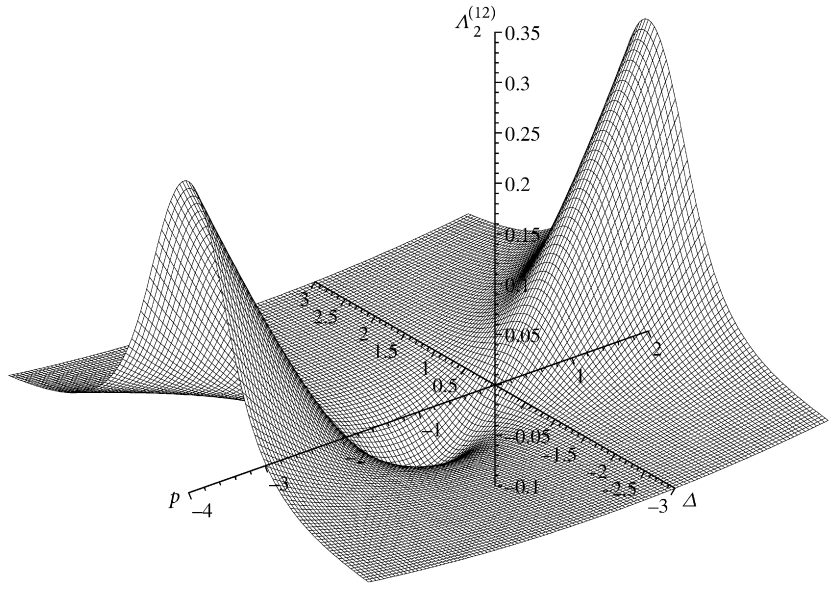

Fig. 2. Second-order perturbation of the moment Lyapunov exponent $\Lambda_2^{(12)}$ ($\sigma = 1.0$).

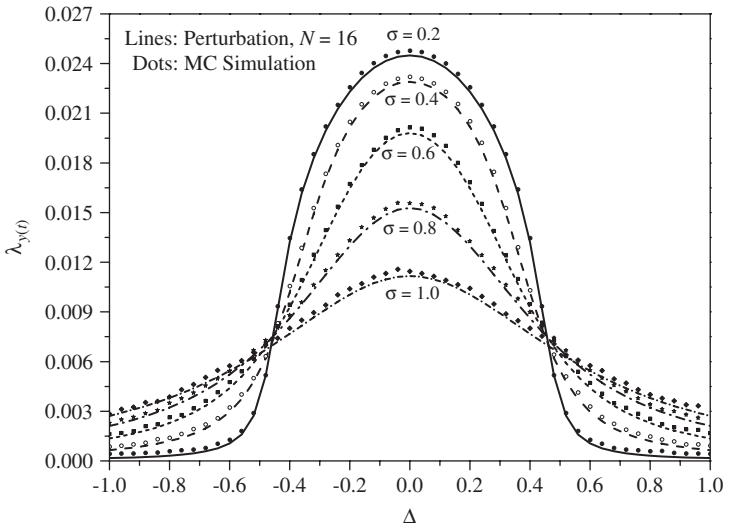

Fig. 3. Comparison of the Lyapunov exponent $\lambda_{y(t)}$ for $\varepsilon = 0.1$, $\beta = 0.5$, and $\mu = 1.0$.

Eq. (26) can be discretized using the Euler scheme, for iterations $k = 0, 1, 2, \ldots$,

$$y_1^k = y_1^{k-1} + y_2^{k-1} \cdot \Delta t$$
$$y_2^k = y_2^{k-1} - [(1 - \varepsilon^2 \mu\beta \cos\eta^{k-1}) y_1^{k-1} + \varepsilon\mu \cos\eta^{k-1} y_2^{k-1}] \cdot \Delta t,$$
$$\eta^k = \eta^{k-1} + v \cdot \Delta t + \varepsilon^{1/2} \sigma \cdot \Delta W^{k-1}.$$

These equations can be simulated iteratively and the numerical algorithm for determining the Lyapunov exponents [25] can be applied to evaluate $\lambda_{y(t)}$. In the Monte Carlo simulation, the time step is chosen as $\Delta t = 0.0005$, and the number of iterations is 10^9. A comparison of the Lyapunov exponents $\lambda_{y(t)}$ obtained using Eqs. (45)–(46) and Monte Carlo simulation as shown in Fig. 3 reveals that there is an excellent agreement between the two results.

A three-dimensional plot of the second-order perturbation of the Lyapunov exponent $\lambda_2^{(16)}$ as obtained using Eq. (46) is shown in Fig. 4. The significant effect of the parametric resonance can be clearly seen for small values of σ.

According to the presented results, the stability of system (24) depends on the values of the damping β and parameters of bounded noise—the amplitude μ, the central frequency v, and the bandwidth σ. The system is unstable if the damping β is negative, which means that energy is fed into the system. The existence of the bounded noise makes the system more unstable. If the damping β is positive, the stability of the system depends on the characteristics of bounded noise. Our main concern here is the primary parametric instability, namely when v is in the vicinity of 2. According to the present analysis, the primary parametric instability may occur when proper values of μ and σ are taken. The parametric instability becomes more significant for larger μ or smaller σ. The Lyapunov exponents can be used to determine the range of the primary parametric instability.

In the following, the results of this section is applied to a single cylinder in cross-flow to study its stability in the lock-in region.

5. Flow-induced instability of a single cylinder in a cross-flow

Stability analysis of the system (22) shows that vortex-induced vibration of a cylinder is a combination of main resonance and parametric instability in the lock-in region. While the lock-in is associated with main resonance, the parametric instability may occur when the parameters of the time-dependent damping component take proper values and become more significant.

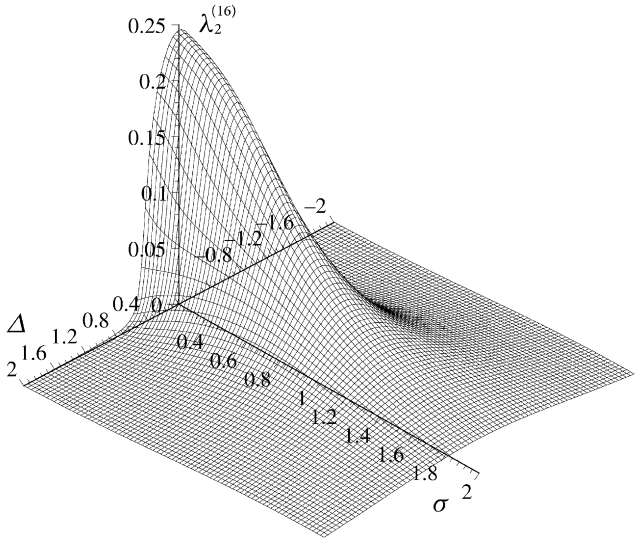

Fig. 4. Second-order perturbation of the Lyapunov exponent $\lambda_2^{(16)}$.

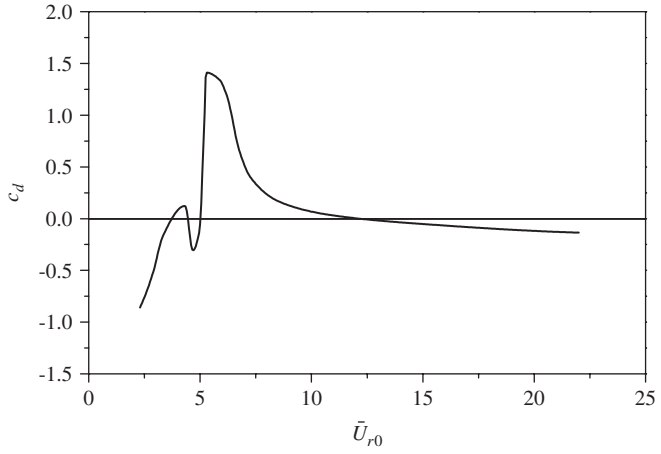

Fig. 5. Fluid damping coefficient c_d for $Re = 2760$ and $d = 1.2$ mm [26].

In the present section, an example is given to demonstrate the behavior of parametric instability. In the example, a rigid cylinder supported by elastic springs and viscous dampers in cross-flow is considered. Reynolds number is set at $Re = 2760$, where data for motion-dependent force coefficients are available in the literature [26]. Fluid inertia coefficients are calculated based on potential flow theory and are approximately unity for all U_{r0} values investigated. Motion-dependent fluid damping and stiffness coefficients are plotted in Figs. 5 and 6, respectively.

According to So et al. [27], the Strouhal number for a stationary cylinder at $Re = 2500$ is $St = 0.2052$, and the rms lift coefficient is $C'_L = 0.68$. These values are assumed for the present case. The mean and rms drag coefficients can be found in Ref. [28], being $\bar{C}_D = 1.0$ and $C'_D = 0.07$, respectively. It is assumed that the bandwidths of both the lift and drag coefficients are equal, being $\tilde{\sigma}_L = \tilde{\sigma}_D = 0.01$. The reduced velocity is varied in the usual lock-in range of $\bar{U}_{r0} = 5.0$ to 6.6, where it is assumed that $\tilde{v}_L \approx 1$ and $\tilde{v}_D = 2\tilde{v}_L \approx 2$. The parameters are chosen so that the vibration level is similar to that reported by Chen et al. [26]. In the present case, the structural damping factor is $\zeta_s = 0.02$, and the mass ratio is varied from $M_r = 15$ to 18 in order to study its effect on the stability.

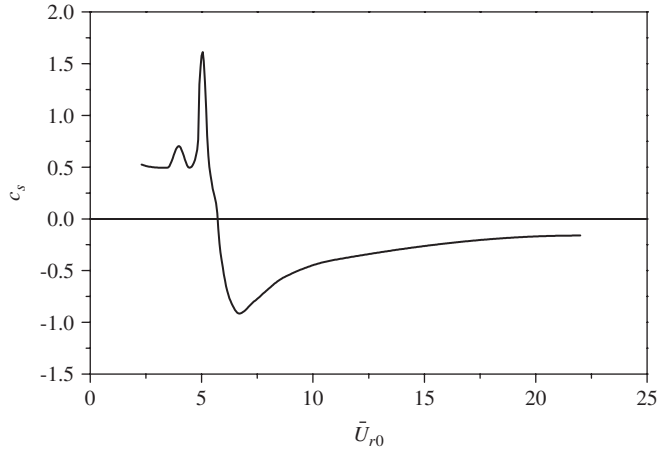

Fig. 6. Fluid stiffness coefficient c_k for $Re = 2760$ and $d = 1.2\,\text{mm}$ [26].

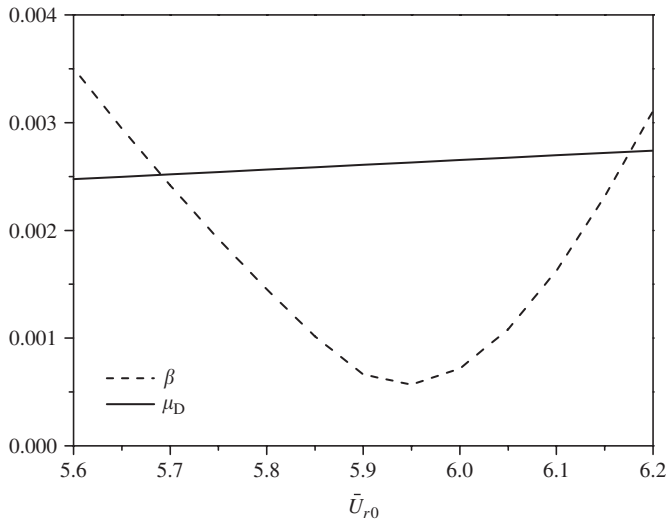

Fig. 7. Values of β and μ_D in the lock-in range for $M_r = 18$, $\zeta_s = 0.02$, $\bar{C}_D = 1.0$, and $C_D = 0.1$.

For $M_r = 18$, the values of β and μ_D as a function of $\bar{U}_{r0}$ are calculated and plotted in Fig. 7. It can be seen that p is positive in the range of $\bar{U}_{r0}$ concerned, hence constant-fluid-damping-induced instability is not present. However, $\mu_D > \beta$ in the range of $\bar{U}_{r0} = 5.6$ to 6.2, so it is possible for parametric instability to occur. In order to study this possibility, the Lyapunov exponents are obtained following the procedure in Section 4, and the results are shown in Fig. 8.

The Lyapunov exponents for system (22) can also be obtained by Monte Carlo simulation. In the simulation, the number of iterations is 2×10^9 and the time step is $\Delta t = 10^{-6}$. The two results shown in Fig. 8 agree with each other quite well.

It can be seen that parametric instability occurs in the range of $\bar{U}_{r0} = 5.85$–6.05. Noting that the usual lock-in range is $\bar{U}_{r0} = 4.0$ to 6.0, it can be seen that parametric instability may co-exist with the main resonance due to lock-in.

When the mass ratio is decreased to $M_r = 17$, the values of β and μ_D as a function of $\bar{U}_{r0}$ are plotted in Fig. 9. It can be seen that this case covers all three situations discussed in Section 3, namely, $\beta < 0$, $\beta > 0$ and $\beta > \mu_D$, $\beta > 0$ and $\beta < \mu_D$. It is seen that $\beta < 0$ for $\bar{U}_{r0} = 5.72$–6.15, suggesting constant-fluid-damping-induced instability occurs in this range. The Lyapunov exponents are calculated and plotted in Fig. 10, from which the

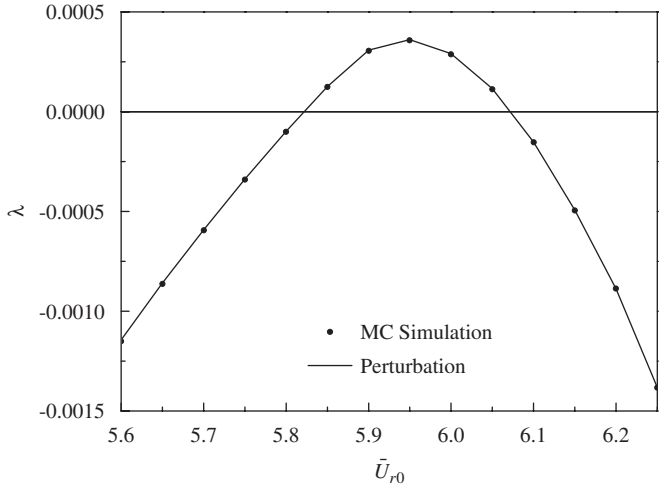

Fig. 8. Lyapunov exponents for $Re = 2760$, $\sigma = 0.01$, $v = 2$, and $M_r = 18$.

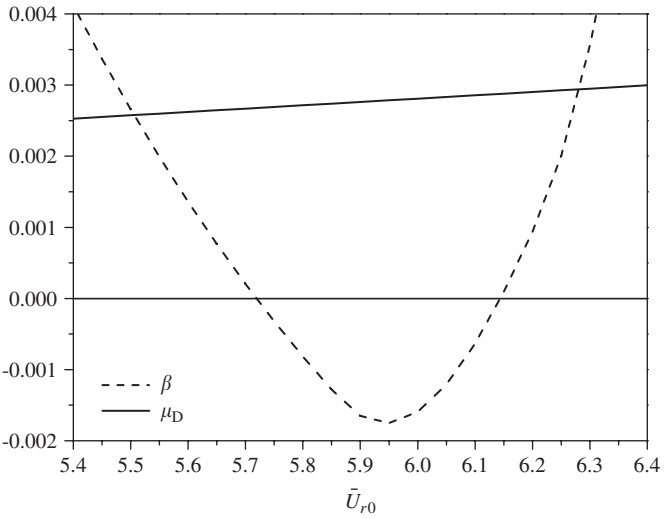

Fig. 9. Values of β and μ_D in the lock-in range for $M_r = 17$, $\zeta_s = 0.02$, $\bar{C}_D = 1.0$, and $C_D = 0.1$.

range of instability is determined to be $U_{r0} = 5.6$–6.22. This means that the parametric resonance enlarges the range of instability. Again, this range overlaps the usual lock-in range. Besides the enlarged instability range, the Lyapunov exponent is bigger than that given by only constant-fluid-damping-induced instability alone. It is clearly shown that the time-dependent fluid-damping component $\mu_D \cos\tilde{\eta}(\tau)$ tends to destabilize the system by enlarging the instability range and enabling the response to increase faster (larger Lyapunov exponent).

In Section 3, it has been shown that the fluid damping coefficient, c_d, is a crucial parameter. In the present example, its effect on parametric instability is studied by varying c_d by $\pm 10\%$ from its original value as reported by Chen et al. [26]. The ranges of instability, as determined by the Lyapunov exponents, for the case $M_r = 17$ and a series of c_d values are shown in Fig. 11. It is seen that the range of instability increases with the increasing of c_d, but decreases when c_d is decreased. It even diminishes as c_d is decreased by 5% or more (the system becomes stable in the whole range of $\bar{U}_{r0}$ considered). This is expected since decreasing c_d will increase β, which leads the system towards stable behavior. When the mass ratio is reduced further to $M_r = 15$, however, the system is always unstable in a certain range of $\bar{U}_{r0}$ regardless of the variation of c_d as shown in Fig. 12. In fact, the effect of decreasing M_r is to destabilize the system, which is clearly shown in Fig. 13.

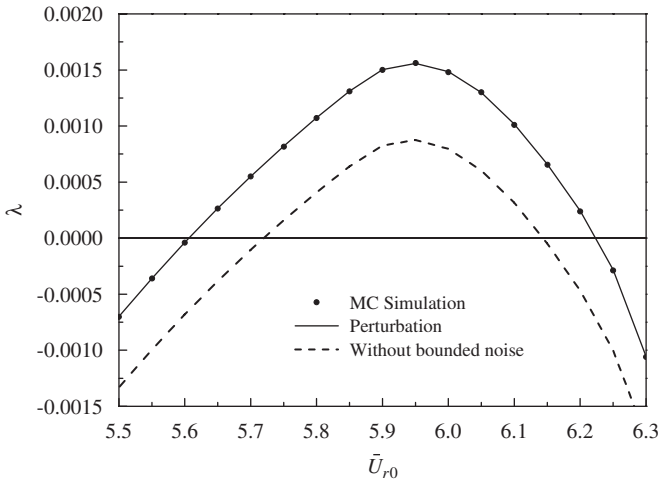

Fig. 10. Lyapunov exponents for $Re = 2760$, $\sigma = 0.01$, $v = 2$, and $M_r = 17$.

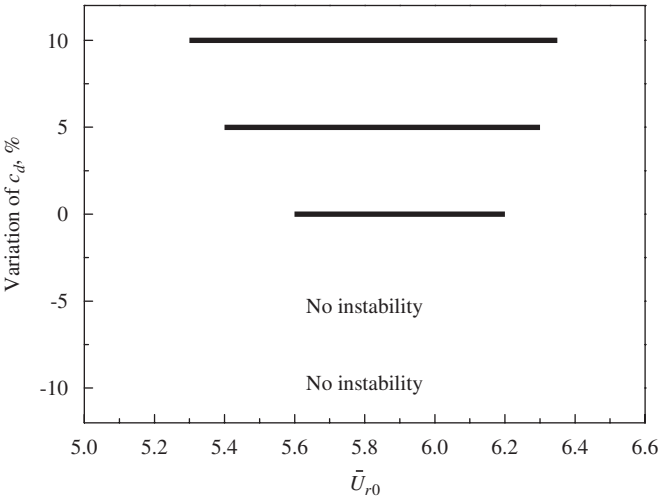

Fig. 11. Stability range with variation of c_d and $M_r = 17$.

This range overlaps partially with the usual lock-in range of U_r from 4.0 to 6.0, suggesting that the large-amplitude vibration of the cylinder observed in the lock-in region could include the contribution of parametric instability. It should be noted that the one-cylinder case is a limiting case of multiple cylinders when the distance between adjacent cylinders is large enough. Hence, it is expected that parametric instability might also play a significant role in flow-induced vibration of multiple cylinders. Therefore, a study of instability of multiple cylinders in a cross-flow is in order.

6. Conclusions

In this paper, a model previously proposed to study vortex-induced vibration of a single cylinder in a cross-flow is extended to include motion-dependent fluid forces, in an attempt to understand its dynamic behavior, especially in the lock-in region. Possible instability is discussed based on the extended model. It is found that, apart from the usual vortex-induced large-amplitude vibration in the lock-in region

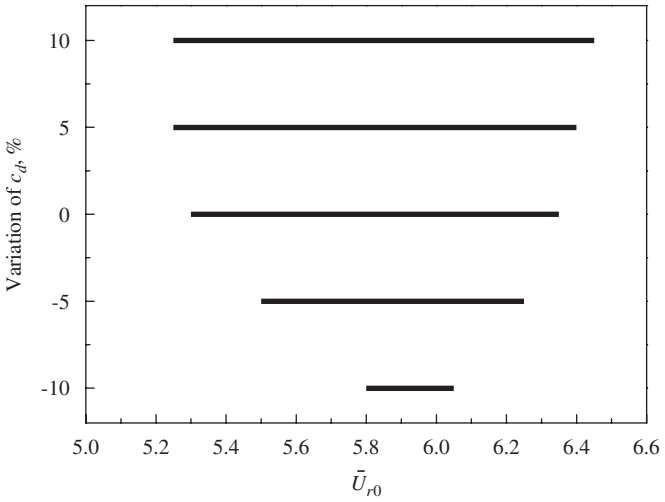

Fig. 12. Stability range with variation of c_d and $M_r = 15$.

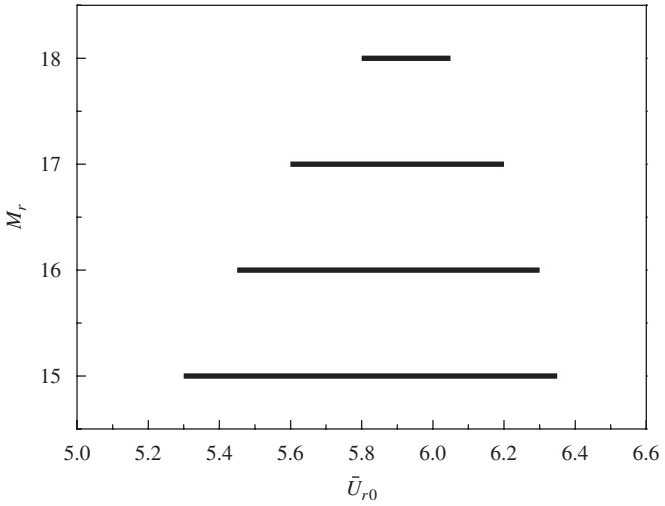

Fig. 13. Stability range with variation of M_r.

and the instability induced by constant fluid-damping force, for which a condition for its occurrence is given, a parametric instability is also possible if the parameters of the system are appropriately selected.

The developed model can be generalized to represent a class of two-dimensional dynamic systems subjected to parametric excitations in the damping term, which is described by a narrow-band bounded noise process. The dynamic stability of the system is studied by determining the moment Lyapunov exponents and the Lyapunov exponents. The partial differential eigenvalue problem governing the moment Lyapunov exponent is established using the theory of stochastic dynamical system. For weak noise excitations, a singular perturbation method is employed to obtain second-order expansions of the moment Lyapunov exponents. The Lyapunov exponent is then obtained using the relationship between the moment Lyapunov exponent and the Lyapunov exponent. The accuracy of the approximate analytical results are validated and assessed by comparing with numerical results. It is observed that there is an excellent agreement between the analytical results and the numerical results.

Based on the stability analysis results of a two-dimensional general dynamic system, an example is given to demonstrate the role of parametric instability in vortex-induced vibration of a single cylinder in a cross flow. When appropriate values of the system parameters are taken, it is shown that the vibration of the cylinder is made up of main resonance due to the lock-in forcing, parametric instability due to time-variant fluid damping, and constant-fluid-damping-induced instability in the usual lock-in range. In particular, the primary parametric resonance enlarges the range of instability. The effects of some crucial parameters, such as the mass ratio and the fluid damping coefficient, are studied. It is shown that decreasing the mass ratio or increasing the constant fluid damping has a positive influence on the instability of the system.

Acknowledgment

Funding supports from the Research Grant Council of the Government of the HKSAR under Project Nos. PolyU5307/03E and PolyU5321/04E are gratefully acknowledged.

References

[1] P. Anagnostopoulos (Ed.), *Vibration induced by vortex shedding*, Flow-induced Vibrations in Engineering Practice, WIT Press, Southampton, UK, 2002, pp. 1–80.
[2] R.D. Gabbai, H. Benaroya, An overview of modeling and experiments of vortex-induced vibration of circular cylinders, *Journal of Sound and Vibration* 282 (2005) 575–616.
[3] T. Sarpkaya, Vortex-induced oscillations — a selective review, *ASME Journal of Applied Mechanics* 46 (1979) 241–258.
[4] T. Sarpkaya, A critical review of the intrinsic nature of vortex-induced oscillations, *Journal of Fluids and Structures* 19 (2004) 389–447.
[5] T. Sarpkaya, Fluid forces on oscillating cylinders, *American Society of Civil Engineers, Journal of the Waterway, Port, Coastal and Ocean Division WW* 4 (1978) 275–291.
[6] O.M. Griffin, G.H. Koopmann, *The Vortex-excited lift and reaction forces on resonantly vibrating cylinders. Journal of Sound and Vibration* 54 (1977) 435–448.
[7] O.M. Griffin, Vortex-excited cross-flow vibrations of a single cylindrical tube, *Transactions of the American Society of Mechanical Engineers, Journal of Pressure Vessel Technology* 102 (1980) 158–166.
[8] S.S. Chen, S. Zhu, Y. Cai, *An unsteady flow theory for vortex-induced vibration.Journal of Sound and Vibration* 184 (1995) 73–92.
[9] R.T. Hartlen, I.G. Currie, *Lift oscillation model for vortex-induced vibration. ASCE Journal of Engineering Mechanics* 96 (1970) 577–591.
[10] R.A. Skop, O.M. Griffin, *A model for the vortex-excited resonant response of bluff cylinders. Journal of Sound and Vibration* 27 (1973) 225–233.
[11] R. Landl, A mathematical model for vortex-excited vibrations of bluff bodies, *Journal of Sound and Vibration* 42 (1975) 219–234.
[12] E. Berger, On a mechanism of vortex excited oscillations of a cylinder, *Journal of Wind Engineering and Industrial Aerodynamics* 28 (1988) 301–310.
[13] S. Balasubramanian, R.A. Skop, Anonlinear oscillator model for vortex shedding from cylinders and cones in uniform and shear flows, *Journal of Fluids and Structures* 10 (1996) 197–214.
[14] X.Q. Wang, R.M.C. So, K.T. Chan, A nonlinear fluid force model for vortex-induced vibration of an elastic cylinder, *Journal of Sound and Vibration* 260 (2003) 287–305.
[15] X.Q. Wang, W.-C. Xie, R.M.C. So, Force evolution model for vortex-induced vibration of one elastic cylinder in cross flow, Proceedings of the 2006 ASME Pressure Vessels and Pipeline Division Conference (PVP2006), July 23–27, 2006,Vancouver, Canada, Paper Number: PVP2006-ICPVT11-93875.
[16] B.J. Vickery, R.I. Basu, Across-wind vibrations of structures of circular cross-section. Part I: development of a mathematical model for two-dimensional conditions, *Journal of Wind Engineering and Industrial Aerodynamics* 12 (1983) 49–73.
[17] W.-C. Xie, Moment Lyapunov exponents of a two-dimensional system in wind-induced vibration under real noise excitation, *Chaos, Solitons and Fractals* 14 (2002) 349–367.
[18] L. Arnold, A formula connecting sample and moment stability of linear stochastic systems, *SIAM Journal of Applied Mathematics* 44 (1984) 793–802.
[19] L. Arnold, E. Oeljeklaus, E. Pardoux, Almost sure and moment stability for linear itô equations. Lyapunov exponents, in: L. Arnold, V. Wihstutz (Eds.), *Lecture Notes in Mathematics*, Vol. 1186, Springer, Berlin, 1986, pp. 85–125.
[20] L. Arnold, W. Kliemann, E. Oeljeklaus, Lyapunov exponents of linear stochastic systems, Lyapunov exponents, in: L. Arnold, V. Wihstutz (Eds.), *Lecture Notes in Mathematics*, Vol. 1186, Springer, Berlin, 1986, pp. 129–159.
[21] L. Arnold, *Random Dynamical Systems*, Springer, Berlin, 1998.
[22] W.-C. Xie, *Dynamic Stability of Structures*, Cambridge University Press, New York, 2006.
[23] W. Wedig, Lyapunov exponent of stochastic systems and related bifurcation problems, in: S.T. Ariaratnam, G.I. Schuëller, I. Elishakoff (Eds.), *Stochastic Structural Dynamics—Progress in Theory and Applications*, Elsevier Applied Science, London, 1988, pp. 315–327.

[24] E. Zauderer, *Partial Differential Equations of Applied Mathematics*, second edn., Wiley, New York, 1989.
[25] A. Wolf, J. Swift, H. Swinney, A. Vastano, *Determining lyapunov exponents from a time series. Physica D* 16 (1985) 285–317.
[26] S.S. Chen, Y. Cai, G.S. Srikantiah, *Fluid damping controlled instability of tubes in crossflow. Journal of Sound and Vibration* 217 (1998) 883–907.
[27] R.M.C. So, Y. Liu, S.T. Chan, K. Lam, *Numerical studies of a freely vibrating cylinder in a cross flow. Journal of Fluids and Structures* 15 (2001) 845–866.
[28] M.M. Zdravkovich, *Flow Around Circular Cylinders*, Vol. 1, Oxford University Press, New York, 1997, pp. 17.